

Degeneracy of non-abelian quantum Hall states on the torus: domain walls and conformal field theory

Eddy Ardonne^{1,2}, Emil J. Bergholtz³, Janik Kailasvuori⁴, and Emma Wikberg³

¹*Center for the Physics of Information, California Institute of Technology, Pasadena, CA 91125, USA*

²*Nordita, Roslagstullsbacken 23, SE-106 91 Stockholm, Sweden*

³*Department of Physics, Stockholm University, AlbaNova University Center, SE-106 91 Stockholm, Sweden*

⁴*Institut für Theoretische Physik, Freie Universität Berlin, Arnimallee 14, 14195 Berlin, Germany*

(Dated: October 22, 2018)

We analyze the non-abelian Read-Rezayi quantum Hall states on the torus, where it is natural to employ a mapping of the many-body problem onto a one-dimensional lattice model. On the thin torus—the Tao-Thouless (TT) limit—the interacting many-body problem is exactly solvable. The Read-Rezayi states at filling $\nu = \frac{k}{kM+2}$ are known to be exact ground states of a local repulsive $k+1$ -body interaction, and in the TT limit this is manifested in that all states in the ground state manifold have exactly k particles on any $kM+2$ consecutive sites. For $M \neq 0$ the two-body correlations of these states also imply that there is no more than one particle on M adjacent sites. The fractionally charged quasiparticles and quasiholes appear as domain walls between the ground states, and we show that the number of distinct domain wall patterns gives rise to the nontrivial degeneracies, required by the non-abelian statistics of these states. In the second part of the paper we consider the quasihole degeneracies from a conformal field theory (CFT) perspective, and show that the counting of the domain wall patterns maps one to one on the CFT counting via the fusion rules. Moreover we extend the CFT analysis to topologies of higher genus.

PACS numbers: 73.43.Cd, 71.10.Pm

I. INTRODUCTION

Microscopic wave functions have ever since Laughlin’s original work [1] back in 1983 been instrumental for the understanding of the fractional quantum Hall effect (FQHE). At Landau level filling fraction $\nu = 1/q$, q odd, Laughlin’s construction shows why an incompressible quantum liquid, with fractionally charged excitations, may form to minimize the electron-electron repulsion by optimizing the short-range correlations as two particles approach each-other. The Moore-Read (MR) [2] and Read-Rezayi (RR) states [3] provide a natural extension of this, where the wave functions vanish as clusters of $k+1$ particles are formed. The latter has filling fraction $\nu = k/(kM+2)$, describing fermions (bosons) for M odd (even).

Conformal field theory (CFT) plays a central role in the theory of the FQHE, as it e.g. describes the edge theory and gives a method for construction of trial wave functions. The understanding of this connection was boosted by Moore and Read with their seminal paper from 1991 [2], where they suggested a general CFT-FQHE connection, and in particular showed that (at least) some FQHE wave functions can be obtained from correlators in certain so called rational CFT’s. Not only did they reproduce the Laughlin wave functions, but also put forward the so called Moore-Read (aka pfaffian) state which supports non-abelian excitations. It was first suggested in [4] that this state can describe the enigmatic state observed [5] at filling $\nu = 5/2$. By now, there is ample (numerical) evidence that this is indeed the case [6, 7, 8]. It is exciting that the first experimental steps towards determining the nature of the $\nu = 5/2$ quantum Hall state have recently been made [9].

Read and Rezayi [10] provided support for the suggestions that the $k=3, M=1$ RR state is underlying the QHE observed at filling $\nu = 12/5$, but the amount of evidence in this case is not as much as for the $\nu = 5/2$ state. However, if this state does indeed describe the $\nu = 12/5$ state, it would open up the fascinating possibility of topological quantum computation, as braiding of the non-abelian excitations would be protected from decoherence by topology and the braid group is rich enough, see e.g. Ref. 11. Recently, another state, with the same non-abelian structure as the MR state, has been proposed to describe the $\nu = 12/5$ QHE [12].

Bosonic RR states have also been predicted to describe the state of a rapidly rotating Bose-Einstein condensate, in the regime where the rotation frequency is so high that the vortex lattice (formed at moderate rotation rates) melts [13]. This system provides a promising environment for these states as the extremely local potentials used to motivate the RR states are more realistic in a dilute atomic bose gas than in the electronic quantum Hall system.

The Read-Rezayi states can be written as (see [14])

$$\Psi_{\text{RR}} = \mathcal{S} \left(\prod_{i_1 < j_1}^{N/k} (z_{i_1} - z_{j_1})^2 \cdots \prod_{i_k < j_k}^{N/k} (z_{i_k} - z_{j_k})^2 \right) \prod_{i < j}^N (z_i - z_j)^M e^{-\frac{1}{4} \sum_i |z_i|^2}, \quad (1)$$

in the disk geometry. Here \mathcal{S} symmetrizes over possible divisions of the particles into k sets of equal size. As already discussed, these states are constructed as CFT correlators. By using the operator product expansions of the fields creating the electrons, one can show that these wave functions are exact ground states of certain local $k + 1$ -body interactions.

On a torus, the topological properties of various QH phases will be manifest. A nice exposition of this can be found in [15]. In particular, the one-dimensional nature of a Landau level is explicit on the torus—a natural set of single-particle states exactly maps the two-dimensional problem onto a one-dimensional lattice model, where all states will be at least q -fold degenerate for states with filling fraction $\nu = p/q$, and fractionally charged excitations naturally appear as domain walls between degenerate ground states [16, 17]. Lately there has been considerable progress in understanding various phases of the QH system in terms of the exactly solvable Tao-Thouless (TT) limit (corresponding to the thin torus), using this mapping. It has been shown that this limit nicely accommodates the gapped hierarchical (abelian) [18, 19, 20, 21], multicomponent liquids [22], as well as gapless fractions [18, 19, 23].

In the present manuscript we extend earlier results [24, 25] obtained for non-abelian FQHE liquids in the TT limit, by considering the thin torus limit of the Read-Rezayi states, in the presence of excitations, by counting the number of TT states on the torus. State counting for non-abelian states has been considered before, and for the MR state, the complete results (on the sphere) appeared in [26]. The first results for the RR states (again for the sphere), appeared in the original paper of Read and Rezayi, in which the states were defined [3]. More general results, in terms of recursion relations, were obtained by Gurarie and Rezayi, [27], by exploiting the results of [28]. Explicit counting formulas were obtained in [29]. More recently, Read [30] constructed an explicit set of wave functions (building on the results of [31]), re-deriving the explicit counting of [29] in the process. The paper [30] also outlines the state-counting on the torus, in terms of character formulas. Subsequently, the quasihole states have been interpreted as Jack polynomials for negative parameter [32, 33], and the orbital occupation numbers used in these two papers are the ones we employ in this work. Our analysis however focusses on the domain walls, which represent the excitations, and the main result is that the domain walls exactly reproduce the structure of the fusion rules of the conformal field theory underlying the Read-Rezayi states.

In particular we show how the number of inequivalent domain walls accounts for the quasiparticle and quasihole degeneracies needed for non-abelian statistics of these states. We also explicitly show that this analysis maps one-to-one on the corresponding CFT analysis of the bulk states, and generalize the counting rules to arbitrary genus.

In section II, we will introduce the thin torus limit of the Read-Rezayi states. States without excitations will be considered first, giving rise to a set of degenerate ground states. The elementary excitations are represented as domain walls between these ground states. The counting of these domain walls will be presented in section II D. In section III, we will revisit this counting from a CFT point of view. We will show that the counting of the domain walls can be mapped one-to-one on the CFT counting, which reveals that the domain walls provide a particularly simple way of representing the fusion rules of CFT.

Some details of the counting are collected in several appendices. Appendix A deals with the generalization of the results to arbitrary M (we assume $M = 0$ in the main text). In Appendix B we explain the connection with the S -matrix. Some of the details of the calculation in section III B are collected in Appendix C. Finally, Appendix D deals with the generalization to arbitrary genus.

II. TAO-THOULESS LIMIT

In this section we describe the Tao-Thouless limit and calculate degeneracies in this solvable limit.

A. One-dimensional description

The structure of a single Landau level on a torus was first worked out by Haldane [34]. Here we provide a simple version that makes the one-dimensional nature of a Landau level explicit.

We consider a (flat space) torus with lengths L_1, L_2 in the x - and y -directions respectively. Consistent boundary conditions can be enforced when $L_1 L_2 = 2\pi N_\phi$ (in units where $\ell = \sqrt{\frac{\hbar c}{eB}} = 1$), where N_ϕ is the number of magnetic flux quanta penetrating the surface. In Landau gauge, $\mathbf{A} = B y \hat{\mathbf{x}}$, the states

$$\psi_j = \pi^{-1/4} L_1^{-1/2} \sum_m e^{i(\frac{2\pi}{L_1} j + m L_2) x} e^{-(y + \frac{2\pi}{L_1} j + m L_2)^2 / 2}, \quad j = 0, 1, \dots, N_\phi - 1, \quad (2)$$

form a basis of one-particle states in the lowest Landau level. ψ_j is quasiperiodic and centered along the line $y = -2\pi j / L_1$. This maps the Landau level onto a one-dimensional lattice model with lattice constant $2\pi / L_1$. A basis

of many-particle states is given by $|n_0, n_1, \dots, n_{N_\phi-1}\rangle$, where n_j is the number of particles occupying site j . Due to periodic boundary conditions, $n_{i+N_\phi} \equiv n_i$. The N -particle problem at filling fraction $\nu = N/N_\phi = p/q$ (p, q coprime) can be shown to be at least q -fold degenerate for any translation invariant interaction.

On the thin torus, the overlap between different single particle states goes to zero, and the interacting many-body problem becomes solvable [18]. For generic interactions, the ground states are regular lattices and the lowest charged excitations appear as domain walls between degenerate ground states. This limit has been termed the Tao-Thouless limit [18, 19] since the exact ground state (for a repulsive two-body interaction) at $\nu = 1/3$ in this limit coincides with the early attempt to explain the quantum Hall effect by Tao and Thouless [35]. It is interesting to note that Anderson, already in 1983, noted that the TT state has a finite overlap with the Laughlin state and he proposed that one can think of the TT state as a 'parent' evolving into the Laughlin state as the interaction is turned on [16].

In the following we will show that Read-Rezayi states have a simple manifestation in this limit and that the counting of quasiparticle (and/or quasihole) states reduces to a combinatorially simple problem.

B. Ground states

Before we study the quasiparticle/quasihole states, we will specify the different ground state sectors. Ground state will in this paper mean a state without quasiparticles and quasiholes (which we will collectively call excitations). (These conventions done here are adapted to the somewhat artificial $k+1$ -body interaction. In the physical situation quasiparticles and quasiholes do not only come as excitations. They are also a necessary part of the ground state when the system deviates from an exact filling fraction.)

We search for the thin torus ground states for the $k+1$ -body interaction at filling $\nu = \frac{k}{kM+2}$. For a given k and M in the TT limit, ground states are those that fulfill the rules

- any $kM+2$ consecutive sites contain exactly k particles
- the distance between two particles is at least M .

The first rule is a consequence of the $k+1$ -body interaction and the filling, and the second rule can be understood from the two-body correlations of the Read-Rezayi states. For $M=0$, the above rules lead to the ground states (in a basis of occupation numbers of the sites)

$$|k-l, l, k-l, l, k-l, l, \dots\rangle, \quad l=0, 1, \dots, k \quad (3)$$

i.e. they have a pattern with the unit cell $[k-l, l]$. For $k=2, M=0$ for example, the possible ground states are $|2020\dots\rangle$, its translated sector $|0202\dots\rangle$, and $|1111\dots\rangle$. For $k=3$ and $M=1$ one such ground state is $|0111001110\dots\rangle$. The unit cells of these sectors are $[20]$, $[02]$, $[11]$ and $[01110]$, respectively. For more examples, see Table I. The sectors are topologically distinct since there is no local process that can transform one sector into the other without passing through states of higher energy.

k	M	TT unit cells	degeneracy
1	2	$[100], \dots$	3
2	0	$[20], [11], \dots$	3 (1)
2	1	$[1100], [1010], \dots$	6 (2)
2	2	$[101000], [100100], \dots$	9 (3)
3	0	$[30], [21], \dots$	4
3	1	$[11100], [11010], \dots$	10
4	0	$[40], [31], [22], \dots$	5 (1)

TABLE I: Examples of ground state sectors in the TT limit. The dots denote that one should complete with all the possible rigid translations of the presented unit cells to get the full space of degenerate ground states and the corresponding degeneracy (for $2N_e/k = 0 \pmod{2}$) to the right. The degeneracies for k even and $2N_e/k = 1 \pmod{2}$ are indicated in brackets and are given by unit cells of the kind $[11]$, $[1010]$, $[22]$ etc, with the reduced periodicity $(kM+2)/2$.

We can now easily reproduce the well known ground state degeneracy on the torus, i.e. the number of ground state sectors, by counting the number of different unit cells. Let us assume that $M=0$ and that the number of sites N_ϕ is even (and hence, $N_e = 0 \pmod{k}$). In that case, all the ground states (3) can be put on a torus (periodic boundary conditions), so the degeneracy is $k+1$. For k even, there is one state which can be put on the torus even when N_ϕ

is odd, namely $|k/2, k/2, k/2, \dots\rangle$. However, this is the only possibility, so the degeneracy is one. For arbitrary M (changing only the center of mass degeneracies), one recovers the results that the degeneracy is $(k+1)(kM+2)/2$ when $2N_e/k = 0 \pmod{2}$, while for $2N_e/k = 1 \pmod{2}$ (only possible for k even) the degeneracy is $(kM+2)/2$.

C. Excitations as domain walls

Excitations are domain walls between different ground state sectors, as in $|11\mathbf{10}202\dots\rangle$. At such domain walls the above rules are not satisfied. An isolated *elementary* excitation is characterized by one string of $kM+2$ consecutive sites carrying $k+1$ or $k-1$ particles, for quasiparticles or quasiholes respectively. An example with $k=2, M=1$:

$$|110011\mathbf{0010}1010\dots\rangle \quad (4)$$

where the only string of $kM+2=4$ sites that has deviating particle content is the string marked in boldface. (Compare e.g. with the adjacent strings starting at the 6th or the 8th site.) In this example, there is a domain wall between the ground state sectors $|1100\dots\rangle$ and $|1010\dots\rangle$ giving a quasihole. We will throughout the paper highlight the strings of deviating particle content in boldface.

To be able to compactly characterize states with domain walls we introduce the following notation. A ground state sector of arbitrary length will be denoted by its unit cell in between square brackets. The unit cell is extracted from the $kM+2$ first sites of the ground states. Thus, for $k=3, M=0$ we have

$$\begin{aligned} |030303\dots\rangle &\rightarrow [03] \\ |121212\dots\rangle &\rightarrow [12] \\ |212121\dots\rangle &\rightarrow [21] \\ |303030\dots\rangle &\rightarrow [30] \end{aligned} \quad (5)$$

A state with domain walls, i.e. with different sectors, is written as a sequence of such unit cells. This is done by comparing each sector with the reference ground states. For $k=3, M=0$ this is illustrated for the last two sectors of the example state $|A\rangle$ below:

$$\begin{aligned} |A\rangle &= |212121\mathbf{1}212121\mathbf{20}3\mathbf{0}3\mathbf{0}2\mathbf{1}2121\rangle \rightarrow [21][12][03][12] \\ &|03030303030303\mathbf{0}3\mathbf{0}3\mathbf{0}3\mathbf{0}3\mathbf{0}303\dots\rangle \rightarrow [03] \\ &|12121212121212\mathbf{1}2\mathbf{1}2\mathbf{1}2\mathbf{1}2\mathbf{1}2\mathbf{1}2\dots\rangle \rightarrow [12]. \end{aligned} \quad (6)$$

This notation in terms of sectors does not specify the state completely, as is seen by states $|A\rangle$ and $|B\rangle$ having the same notation;

$$\begin{aligned} |A\rangle &= |212121\mathbf{1}212121\mathbf{20}3030\mathbf{0}212121\rangle \rightarrow [21][12][03][12] \\ |B\rangle &= |2121\mathbf{2}21212121\mathbf{1}3030\mathbf{0}212121\rangle \rightarrow [21][12][03][12] \end{aligned} \quad (7)$$

though the first domain wall in $|A\rangle$ is a quasihole and the first domain wall in $|B\rangle$ on the other hand is a quasiparticle. However, one can make the notation unambiguous (up to the length of the intermediate sectors) by specifying the charge of each domain wall (i.e. if it corresponds to a quasihole or quasiparticle). However, for the non-abelian structure this ambiguity is immaterial, wherefore the compact notation is useful for us. Nevertheless, as we will see later, the constraint on the number of particles does depend on whether we have quasiparticles, quasiholes or a mixture.

It is important to notice that not any pair of sectors would give a domain wall that corresponds to an elementary excitation. Again, we stress that an elementary excitation is characterized by a single string containing $k\pm 1$ particles for quasiparticles and quasiholes respectively. Taking $k=3, M=0$ as an example, starting from the sector $|2121\rangle$, the only elementary excitations are given by the domain walls (given in both notations, with the quasiholes on the left and the quasiparticles on the right)

$$\begin{aligned} |2121\mathbf{1}21212\dots\rangle &\rightarrow [21][12] & |2121\mathbf{2}21212\dots\rangle &\rightarrow [21][12] \\ |2121\mathbf{20}3030\dots\rangle &\rightarrow [21][30] & |2121\mathbf{30}3030\dots\rangle &\rightarrow [21][30]. \end{aligned}$$

On the other hand the domain wall $|2121\mathbf{0}3\dots\rangle$ (i.e. $[21][03]\dots$) is not of elementary charge. In general we have for $M=0$ (for $M\neq 0$, see Appendix A) that only the following domain walls correspond to elementary excitations:

$$[k-l, l][k-l-1, l+1] \quad [k-l, l][k-l+1, l-1] \quad \text{for } 0 < l < k \quad (8)$$

$$[k, 0][k-1, 1] \qquad [0, k][1, k-1] . \qquad (9)$$

The charge of the elementary excitations, for general M , is $e^* = \pm \frac{e}{kM+2}$ (the charge of the particles is set to e). This can be determined by the Su-Schrieffer counting argument [36]. Here we present an alternative way to derive the charge of the excitations, which can be applied to general filling fractions $\nu = \frac{p}{q}$ (given the ground states), and which does not require any particular number of quasiparticles/holes. There are in total N_ϕ strings of $kM+2$ consecutive sites, one starting at each of the N_ϕ sites. In the absence of excitations, the density within each string would be $k/(kM+2)$ particles per site and the total charge of the ground state would be

$$eN_e = N_\phi \times \frac{ek}{kM+2} .$$

In the presence of n_{qp} quasiparticles and n_{qh} quasiholes, on the other hand, each excitation contributes with one string of deviating density and one has a total charge

$$eN_e = (N_\phi - n_{qp} - n_{qh}) \frac{ek}{kM+2} + n_{qp} \frac{e(k+1)}{kM+2} + n_{qh} \frac{e(k-1)}{kM+2} . \qquad (10)$$

$(N_\phi - n_{qp} - n_{qh})$ is the number of strings with the original ground state density. Rewriting this expression we find

$$eN_e = N_\phi \frac{ek}{kM+2} + (n_{qp} - n_{qh}) \frac{e}{kM+2} , \qquad (11)$$

from which one reads off the charge of the excitations:

$$e^* = \pm \frac{e}{kM+2} .$$

Note that (11) determines the number of flux quanta, which is integer. This gives a constraint on the number of particles, quasiparticles and quasiholes.

D. Degeneracy in the presence of excitations

We will now calculate the degeneracy of the Read-Rezayi states in the presence of excitations in the TT limit. For the nontrivial part of the calculation it is enough to study the bosonic $M=0$ case, because adding an overall Jastrow factor to the wave function can not change the degeneracy related to the non-abelian statistics. The reasons for this from the thin-torus point of view are explained in Appendix A.

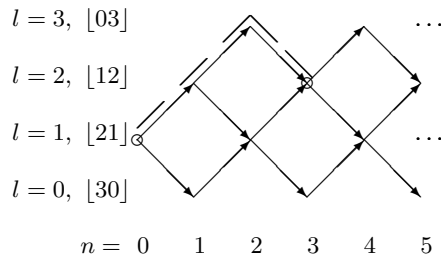


FIG. 1: An example of a Bratteli diagram, here for those $k=3$, $M=0$, states that has $[21]$ as starting sector. The arrows indicate which sectors one can go to from a previous one to get a domain wall of elementary charge. The circles are added just to guide the eye for the example discussed in the text. The sequences in (7) would be represented by the path indicated by the dashed line.

Concentrating on the case $M=0$ from now on, the degeneracy of the general state containing n_{qp} elementary quasiparticles and n_{qh} elementary quasiholes is given by the number of distinct sequences of $n = n_{qp} + n_{qh}$ domain walls as in the examples to the right in (7). Such sequences can be represented by Bratteli diagrams as in Fig. 1,

where the arrows stand for possible domain walls of elementary charge according to (8). In Section III we will see that the same structure appears from the CFT perspective.

Let us consider the simple example of Fig. 1. The l designate the *levels* in the diagram. For $M = 0$ each level can be characterized by one sector. From the diagram we infer that for $n = 3$ domain walls there is no sequence of sectors leading back to the starting sector [21]. (Note that ending with the same sector would impose $N_\phi = \text{even}$.) However, there are three paths from [21] at $n = 0$ to its translated sector [12] at $n = 3$. (All the allowed paths between the two circles.) By terminating [12] in the middle of its unit cell (hence $N_\phi = \text{odd}$) as done in (6), periodic boundary conditions can be fulfilled. Other states with three domain walls and N_ϕ odd can be found by starting with any of the other sectors [30], [12] or [03] and drawing the same kind of diagram. With the choice [12] the result will of course again be three paths, whereas starting with [30] and hence terminating with [03] (or vice versa) gives only one. The torus degeneracy td for $N_\phi = \text{odd}$, $k = 3$ and $M = 0$ is the sum of all different possibilities for $n = 3$ domain walls, resulting in $td = 8$. For $N_\phi = \text{even}$, on the other hand, $td = 0$ in this case.

These calculations can be formalized by introducing the off-diagonal $(k + 1) \times (k + 1)$ adjacency matrix \mathbf{N}_1 with $(N_1)_{ij} = \delta_{i,j+1} + \delta_{i,j-1}$; $i, j = 0, \dots, k$. It readily follows that the number of distinct paths $d(k, n, l_1, l_2)$ starting at level l_1 and terminating at level l_2 via n domain walls is given by the matrix element of the n^{th} power of the adjacency matrix;

$$d(k, n, l_1, l_2) = (N_1^n)_{l_1 l_2}. \quad (12)$$

The total degeneracy is given by the sum of all allowed paths that also are compatible with the periodic boundary conditions. When the number of sites, N_ϕ , is even, these paths are the ones with $l_1 = l_2$, and when N_ϕ is an odd number, they are the ones that connect level l_1 with its complementary level $l_2 = k - l_1$. Combining this we find the total degeneracy to be

$$td(k, M = 0, n, \delta) = \sum_{\text{paths}} d(k, n, l_1, l_2) = \text{Tr}(\mathbf{N}_1^n \mathbf{B}^\delta). \quad (13)$$

Here $\delta = 0$ when the sequence returns to its initial level, i.e. $l_2 = l_1$ (N_ϕ even) whereas $\delta = 1$ when the sequence terminates at the complementary level $l_2 = k - l_1$ (N_ϕ odd). The off-diagonal permutation matrix $(B)_{ij} = \delta_{i,k-j}$; $i, j = 0, \dots, k$ connects the complementary levels.

For $M = 0$, (11) yields $N_\phi = (2N_e + n_{\text{qh}} - n_{\text{qp}})/k$, thus $\delta = (2N_e + n_{\text{qh}} - n_{\text{qp}})/k \bmod 2$. However, M only affects the center of mass degeneracy, hence this expression for δ holds generically (see also Appendix A). Thus, for general M , we find

$$td(k, M, n, \delta) = \frac{kM + 2}{2} \text{Tr}(\mathbf{N}_1^n \mathbf{B}^\delta), \quad (14)$$

with $\delta = (2N_e + n_{\text{qh}} - n_{\text{qp}})/k \bmod 2$. For odd k one can also write $\delta = n \bmod 2$ (obvious from inspection of pertinent Bratteli diagrams) and hence replace \mathbf{B}^δ in (14) by \mathbf{B}^n since $\mathbf{B}^2 = 1$. For even k one can insert domain walls only in pairs, which the result (14) captures by giving $td = 0$ for odd n .

We arrived at this formula for the degeneracy of the Read-Rezayi states on the thin torus by considering the simple picture of domain walls representing the elementary excitations. As we will see in section III, this formula exactly reproduces the counting formula one obtains by using more sophisticated conformal field theory methods, which were used to define the Read-Rezayi states. We will also show how the trace in (14) can be evaluated, with the result given in (31).

It is however instructive to consider a few simple examples explicitly, which can be obtained by evaluating the trace. We will compare these torus degeneracies with the degeneracies on the plane¹, namely $pd(k, M, n, \delta = 0) = d(k, n, 0, 0)$ and $pd(k, M, n, \delta = 1) = d(k, n, 0, k)$:

$$td(2, M, n, \delta) = \frac{2M + 2}{2} (2^{n/2+1} + (-1)^\delta \delta_{n,0}) \quad pd(2, M, n, \delta) = (2^{n/2} + (-1)^\delta \delta_{n,0}) \quad (15)$$

$$td(3, M, n) = \frac{3M + 2}{2} 2(\mathcal{F}_{n-1} + \mathcal{F}_{n+1}) \quad pd(3, M, n) = \mathcal{F}_{n-1} \quad (16)$$

$$td(4, M, n, \delta) = \frac{4M + 2}{2} (2(3^{n/2} + (-1)^\delta) + \delta_{n,0}) \quad pd(4, M, n, \delta) = ((3^{n/2-1} + (-1)^\delta)/2 + \delta_{n,0}/3), \quad (17)$$

¹ The results for the plane were also given in [37], a nice paper in which the braid properties of the RR quasiholes are calculated.

where it is assumed that n is even for even k . \mathcal{F}_n are the Fibonacci numbers, $\mathcal{F}_n = \mathcal{F}_{n-1} + \mathcal{F}_{n-2}$, with the initial conditions $\mathcal{F}_0 = 0$ and $\mathcal{F}_1 = 1$.

In general, one can write the torus degeneracies in terms of recursion relations. Taking $k = 5$, $M = 0$ as an example, one finds the following result: $td(5, 0, n) = td(5, 0, n-1) + 2td(5, 0, n-2) - td(5, 0, n-3)$, with the initial conditions $td(5, 0, 0) = 6$, $td(5, 0, 1) = 2$ and $td(5, 0, 2) = 10$.

III. COUNTING FROM A CONFORMAL FIELD THEORY PERSPECTIVE

In this section, we will show that there is a very close connection between the counting of the states on the thin torus and conformal field theory. We will do this by performing the counting in a conformal field theory setting in a rather (perhaps overly) explicit way. This section is written for an audience which is not too familiar with conformal field theory, and would like to understand some of the ideas underlying the state counting by making use of CFT techniques. As a remark for the experts, one could express the results directly in terms of the modular S -matrix, which diagonalizes the fusion rules [38]. However, doing the calculation in a more explicit way nicely reveals the connection with the thin-torus limit. This also has the advantage that we can easily deal with the case $\delta = 1$ (see the previous section), which is more complicated in terms of the S -matrix. In appendix B we will make some general remarks about expressing the counting in terms of the S -matrix.

A. General remarks

We will start by explaining the origin of the degeneracy on the plane² and torus in general terms, before going into the details of the specific case at hand. The conformal field theory, which can be used to describe (or define) quantum Hall states, contains a set of (primary) fields ϕ_a , which one can think of as the creation operator of particles of type ‘ a ’. In order to be a consistent theory, there has to be an ‘identity’ particle (the vacuum). In addition, for each particle a , there has to be a dual (or anti-) particle, which we denote by \bar{a} . As a simple example, we consider the description of the $\nu = 1/3$ Laughlin state. This theory contains three particle types; ϕ_0 , ϕ_1 and ϕ_2 , with charges 0, $e/3$ and $2e/3$. One can combine two particles with charge $e/3$ into one particle with charge $2e/3$ by bringing them close together, or in other words, by ‘fusing’ the two particles. In taking an electron completely around any of the three types of particles, one does not pick up any nontrivial phase. In this sense, the electrons are trivial, and correspond to the ‘identity’ sector. Thus, in this theory, charge is defined modulo e . We can now specify the rules stating how particles can be combined, the so called fusion rules. In this case, they are simply given by $\phi_i \times \phi_j = \phi_{i+j \bmod 3}$.

The fusion rules in an abelian theory are of the form $\phi_a \times \phi_b = \phi_c$. However, fusing two particles in a non-abelian theory in general gives more than one possible result. This possibility lies at heart of the degeneracies studied in this paper. In general, the fusion rules can be written as

$$\phi_a \times \phi_b = \sum_c (N_a)_{b,c} \phi_c, \quad (18)$$

where the integer $(N_a)_{b,c}$ is the number of times ϕ_c appears in the fusion of the fields ϕ_a and ϕ_b (note that a more conventional notation would be $N_{a,b}^c$). In this paper, we only consider theories for which $(N_a)_{b,c} = 0, 1$. In this case, it is easy to represent the fusion rules in a graphical way. The particles are represented by lines, which are labeled by the particle type. The ‘graph’ in Fig. 2 means that two particles of type a and b can fuse to a particle of type c . The

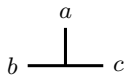


FIG. 2: Graphical representation of the fusion rule.

fusion of more than two particles is represented similarly. For instance, fusing three particles a , b and c to a particle

² The results on the sphere are the same, if one considers localized excitations. In the numerical studies of quantum Hall states on the sphere, this is not the case if one only fixes the flux, number of electrons and their interaction. In this case, the counting is more complicated, see for instance [29].

of type d , namely³

$$(\phi_a \times \phi_b) \times \phi_c = \sum_{d,e} (N_b)_{a,e} (N_c)_{e,d} \phi_d, \quad (19)$$

is shown in Fig. 3. Note that in a non-abelian theory, there can be more than one consistent way of labelling this graph, i.e. the label e can take more than one value.

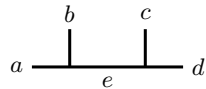


FIG. 3: Fusion of the three particles a , b and c .

After these general remarks, we will now focus on the Read-Rezayi states, but leave the details for the next section. Fusing n quasiholes, which we will denote by ϕ_1 , leads to

$$\phi_1 \times \phi_1 \times \cdots \times \phi_1 = \sum_{\{a_i\}} (N_1)_{1,a_1} (N_1)_{a_1,a_2} \cdots (N_1)_{a_{n-2},a_{n-1}} \phi_c = (N_1^{n-1})_{1,c} \phi_c. \quad (20)$$

As we will show in the following section, the matrix \mathbf{N}_1 describing the fusion of the quasiholes (or quasiparticles) in the Read-Rezayi states is exactly the same matrix describing the possible domain walls between the different sectors. Thus, the rules for domain walls exactly reproduce the fusion rules associated with the Read-Rezayi states! This observation lies at heart of the close connection between the Tao-Thouless states and (the combinatorics of) conformal field theory.

To make this connection more concrete, we consider the degeneracy of the states with n quasiholes on the plane. In general, one has to count the number of different ways in which one can fuse all the fields to the identity. This condition is the non-abelian generalization of charge neutrality. Taking the case $k = 3$, with $n = 6$ quasiholes as an example, this degeneracy is given by the number of labellings of the fusion graph on the left in Fig. 4. Each possible labelling of this graph uniquely corresponds to a path on the Bratteli diagram on the right.

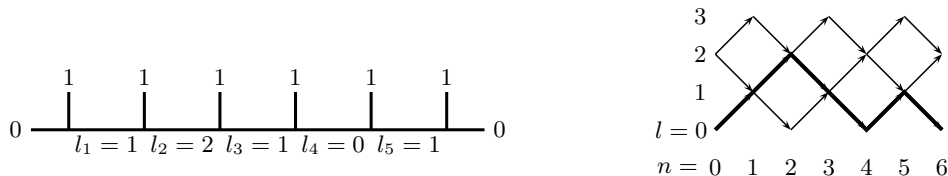


FIG. 4: The connection between the labellings of the fusion graph and the paths on a Bratteli diagram. The labels $\{l_i\}$ on the fusion graph correspond to the bold path on the Bratteli diagram.

On the torus, the situation is slightly different. In this case, one can create a particle-hole pair b and \bar{b} and take one of them, say b , around one of the handles of the torus. Then, one could successively fuse all the n quasiholes with the particle b , and finally annihilate the resulting particle with \bar{b} . Following this logic, the degeneracy on the torus (in the case that $\delta = 0$, see the previous section) is given by the number of labellings of the graph of Fig. 5. Because all the

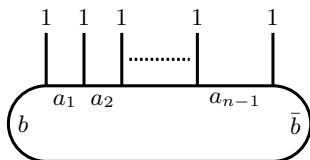


FIG. 5: The number of consistent labellings $\{b, \bar{b}, a_i\}$ of this graph is the torus degeneracy.

³ One can also first fuse particle b with c , and the resulting particle with a . Requiring that the two results are the same gives the associativity condition on the fusion matrices.

possible particles b are self-dual (as explained in the following section), it follows that to obtain the degeneracy on the torus, one has to count all the paths on the Bratteli diagram, which begin and end at the same value of l , see Fig. 4. Thus, the torus degeneracy (in the case $\delta = 0$) is given by $\sum_l (N_1^n)_{l,l} = \text{Tr}(\mathbf{N}_1^n)$, i.e. equation (13). Once again, we see that the structure of the domain walls in the thin-torus limit precisely reproduces the results obtained by using the fusion rules. Thus, one can interpret the domain walls as a very elegant representation of the fusion rules.

B. Counting of the Read-Rezayi states on the torus

We will now move on to the details of the counting of the torus degeneracy of the Read-Rezayi states in the presence of quasipoles (note that we could also consider quasiparticles without additional complication). We will use the fact that the operators creating the electrons and the quasipoles can be written in terms of fields of the \mathbf{Z}_k parafermion theory (see [39]) in combination with a vertex operator, constructed from a compactified chiral boson. In fact, this is the way these states were originally constructed [3]. The vertex operator is purely abelian, and does not contribute to the degeneracy associated with the quasipoles, so we will concentrate on the parafermion part of the theory for now. Of course, the chiral boson will play a role in the center of mass degeneracy later on.

We will think of the \mathbf{Z}_k parafermion theory in terms of the $su(2)_k/u(1)_{2k}$ coset theory. Hence, the parafermion fields Φ_m^l are labeled by an $su(2)$ label l , which takes values $l = 0, 1, \dots, k$ and a $u(1)$ label m , taking values $m = 0, 1, \dots, 2k - 1$. Because the $u(1)$ theory is at level $2k$, or radius $\sqrt{2k}$, the label m is defined modulo $2k$, i.e. we have the following identification:

$$\Phi_m^l \equiv \Phi_{m+2k}^l . \quad (21)$$

Furthermore, from the coset construction, it follows that the labels l and m have to be ‘compatible’, which in the case at hand means that $l + m = 0 \pmod k$. Finally, the requirement that the coset theory is modular yields the following field identification [40]:

$$\Phi_m^l \equiv \Phi_{m+k}^{k-l} . \quad (22)$$

From this it follows that the \mathbf{Z}_k theory has $k(k+1)/2$ primary fields, and the fusion rules of the theory are determined by the fusion rules of the $su(2)_k$ theory which take the following form:

$$\Phi_{m_1}^{l_1} \times \Phi_{m_2}^{l_2} = \sum_{l_3=|l_1-l_2|}^{\min(l_1+l_2, 2k-l_1-l_2)} \Phi_{m_1+m_2}^{l_3} , \quad \text{with } l_3 = l_1 + l_2 \pmod 2 . \quad (23)$$

The parafermion fields ψ_i , with $i = 0, 1, \dots, k-1$, are given by $\Phi_{2i}^0 \equiv \Phi_{2i-k}^k$. Their conformal dimension is $h_{\psi_i} = \frac{i(k-i)}{k}$ and they have abelian fusion rules $\psi_{i_1} \times \psi_{i_2} = \psi_{i_1+i_2}$. The spin fields $\sigma_i \equiv \Phi_i^i$ have scaling dimension $h_{\sigma_i} = \frac{i(k-i)}{2k(k+2)}$.

We can now specify the operators creating the electrons and (elementary) quasipoles for the Read-Rezayi states [26]. For convenience, we give the explicit form of these operators for the Moore-Read pfaffian state ($k = 2$) on the right, by using the operators ψ and σ of the Ising CFT.

$$V_{\text{el}}(z) = \Phi_2^0(z) e^{i\sqrt{(kM+2)/k}\varphi_c(z)} \quad V_{\text{el,mr}}(z) = \psi(z) e^{i\sqrt{M+1}\varphi_c(z)} \quad (24)$$

$$V_{\text{qh}}(w) = \Phi_1^1(w) e^{i\sqrt{k(kM+2)}\varphi_c(w)} \quad V_{\text{qh,mr}}(w) = \sigma(w) e^{i\sqrt{4(M+1)}\varphi_c(w)} , \quad (25)$$

where φ_c is a chiral boson, which creates the charge of the electron and quasipole. From the point of view of the state counting, one can write the operator creating quasiparticles in the MR state (and similarly in the RR states) as $V_{\text{qp}}(w) = \sigma(w) e^{-i\sqrt{4(M+1)}\varphi_c(w)}$, though this operator would not give sensible wave functions. Nevertheless, this operator can be modified in such a way to give explicit wave functions in the presence of quasiparticles [41].

The wave functions of the Read-Rezayi states can be expressed in terms of correlators of the operators V_{el} and V_{qh} ;

$$\Psi_{\text{RR}} = \langle V_{\text{el}}(z_1) \cdots V_{\text{el}}(z_{N_e}) V_{\text{qh}}(w_1) \cdots V_{\text{qh}}(w_{n_{\text{qh}}}) \mathcal{O}_{\text{bg}} \rangle , \quad (26)$$

where \mathcal{O}_{bg} is a background operator ensuring $u(1)$ -charge neutrality. The z_i and w_i are the (complex) positions of the electrons and quasipoles respectively. The form of the wave functions without quasipoles was first given in [3]. To obtain the wave functions for an arbitrary number of quasipoles is hard, but for four quasipoles (in which case there are two conformal blocks), they were explicitly calculated in Ref. 42.

To obtain the degeneracy of the Read-Rezayi states on the torus, in the presence of quasiholes, we have to count the number of consistent labellings of the fusion graph shown in Fig. 6. The solid lines numbered $1, \dots, n_{\text{qh}}$ represent the spin field Φ_1^1 , which is associated with the quasiholes. The dashed lines represent the electrons, and correspond to the field Φ_2^0 . The labels a_i and b have to be chosen consistently with the fusion rules. The lines ‘connecting’ the dashed lines representing the electrons do not have a label, because they are completely determined by the fusion rules. Fusing an electron with an arbitrary particle always gives a unique result. We will concentrate on the bosonic

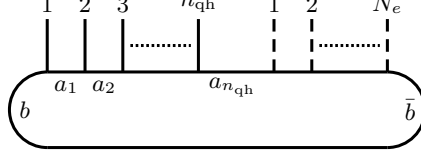


FIG. 6: The number of consistent labellings of this graph is the torus degeneracy.

$M = 0$ case first. So, we are dealing with the $su(2)_k$ theory, which has $k + 1$ fields that are all self-dual, i.e. $a = \bar{a}$, or in other words, the fusion rules are of the form $a \times \bar{a} = \mathbf{1} + \dots$. This implies that the label b in Fig. 5 can take $k + 1$ different values.

Because we will be considering the insertion of electrons, which are described by descendent fields (namely, of the identity), it turns out that the full counting is most easily done in terms of the parafermion fields. This also allows us to deal with the case $\delta = 1$ as well. In terms of the parafermions, the possible labellings of b are $\Phi_{l \bmod 2}^l$, with $l = 0, 1, \dots, k$. Modulo the chiral boson factors, which do not affect the counting, these fields are self-dual. This implies a constraint on the number of quasiholes and electrons. Namely, the $u(1)$ labels of all the inserted fields have to sum to zero, modulo $2k$. Thus, naively one would get the constraint that $2N_e + n_{\text{qh}} = 0 \bmod 2k$. However, by making use of the field identification (22), we actually find that consistent labellings are possible when $2N_e + n_{\text{qh}} = 0 \bmod k$, which is precisely the condition that the number of flux quanta is an integer. From this condition, it follows that for k even, n_{qh} also has to be even.

We continue by focussing on the $su(2)$ label l of the parafermion fields. Fusing a field with a quasihole will change this label by one, i.e. it flips the parity:

$$\Phi_1^1 \times \Phi_m^l = \Phi_{m+1}^{l-1} + \Phi_{m+1}^{l+1}, \quad (27)$$

where the first and the second field on the right hand side are present only if $l - 1 \geq 0$ or $l + 1 \leq k$, respectively. The corresponding fusion matrix is given by $(N_1)_{b,c} = \delta_{b,c-1} + \delta_{b,c+1}$, where $b, c = 0, 1, \dots, k$. The only other way to change the label l is by making use of the field identification (22). This will only change the parity of the label l in the case that k is odd. Fusing with an electron, namely Φ_2^0 , does not change l . Because all the fields $\Phi_{l \bmod 2}^l$ are self-dual, it follows that $b = \bar{b}$. Thus, if b takes the value $\Phi_{l \bmod 2}^l$, we find the condition that after fusing this field with all the n_{qh} quasiholes, and a possible application of the field identification (22), we should end up with a parafermion field with the $su(2)$ label l . This field should be fused with the right number of electrons, such that the resulting field is \bar{b} . In this way, we find the consistent labellings of the graph in Fig. 6. Note that the number of electrons is determined by the relation $2N_e + n_{\text{qh}} = 0 \bmod 2k$ when the field identification is not used (this corresponds to the case $\delta = 0$ in the previous section), or $2N_e + n_{\text{qh}} = k \bmod 2k$, when it is (i.e., $\delta = 1$). Note that there are combinations of the number of electrons and quasiholes for which neither of these conditions is satisfied. In those cases, no states exist.

Let us focus on the case $2N_e + n_{\text{qh}} = 0 \bmod 2k$ first, i.e. we do not make use of the field identification. This can occur for k odd and n_{qh} even, or when both k and $(2N_e + n_{\text{qh}})/k$ are even. In both cases, we fuse with an even number of quasiholes, from which it follows that there is a parafermion field with label l in the possible fusion outcomes.

We will now explain the connection between the labellings of the graph in Fig. 6 and the number of paths on the Bratteli diagrams given in section IID. Let us say we start with a field Φ_m^l . Fusing with a quasihole, or Φ_1^1 , can only give two possible results, namely the ‘neighbouring’ fields Φ_{m+1}^{l-1} and Φ_{m+1}^{l+1} , which are the possibilities for the intermediate label a_1 . In the Bratteli diagram, this corresponds to the two possible directions, starting from the level l (assuming that $0 < l < k$). Repeating this, one finds the correspondance we were after.

Recall that we denote the number of paths on the level k Bratteli diagram, starting at l_1 and ending, after fusing n_{qh} quasiholes, at l_2 by $d(k, n_{\text{qh}}, l_1, l_2)$. This number is given by $(N_1^{n_{\text{qh}}})_{l_1, l_2}$. The number of fusion paths in the case at hand is given by $d(k, n_{\text{qh}}, l, l)$. To obtain the degeneracy on the torus, we have to sum over all possible values of b , or, in other words, l , so the degeneracy is given by $\sum_{l=0}^k d(k, n_{\text{qh}}, l, l)$. In other words, the total number of states is given by the trace of the n_{qh} -th power of the fusion matrix \mathbf{N}_1 , or equivalently, by the sum of all eigenvalues raised to the power n_{qh} . In Appendix C, it is shown that the eigenvalues in this case are given by $2 \cos\left(\frac{(l+1)\pi}{k+2}\right)$, with $l = 0, 1, \dots, k$.

So, in the case that $2N_e + n_{\text{qh}} = 0 \pmod{2k}$, we find that the number of n_{qh} quasihole states on the torus is given by

$$\sum_{l=0}^k \left(2 \cos\left(\frac{(l+1)\pi}{k+2}\right) \right)^{n_{\text{qh}}}. \quad (28)$$

Let us now consider the case $2N_e + n_{\text{qh}} = k \pmod{2k}$, where we do make use of the field identification (22). This case can occur when both k and n_{qh} are odd or when k is even and $(2N_e + n_{\text{qh}})/k$ is odd. When both k and n_{qh} are odd, we need to make use of the field identification, because otherwise no parafermion field with $su(2)$ label l is present in the fusion of the field b and the quasiholes. When k is odd, but $(2N_e + n_{\text{qh}})/k$ even, using the field identification does not change the parity of l , so after the field identification, the field with label l will be present. In the Bratteli diagram, the label l occurs at ‘level’ l . However, after using the field identification, the ‘level’ at which the label l occurs is $k-l$. Thus, to obtain the torus degeneracy in the case the field identification is used, we need to know the number of paths on the Bratteli diagram which start at l , and end at $k-l$, and sum over them, i.e. $\sum_{l=0}^k d(k, n_{\text{qh}}, l, k-l)$.

In Appendix C, we will explain how to calculate this sum and here we will simply quote the result:

$$\sum_{l=0}^k (-1)^l \left(2 \cos\left(\frac{(l+1)\pi}{k+2}\right) \right)^{n_{\text{qh}}}. \quad (29)$$

The only difference with formula (28) is the additional sign, which can be explained as follows. In this case, we have an odd number of flux quanta. In transporting one of the particles of the particle-hole pair around one of the handles of the torus, one can pick up a sign, which happens in the case that b corresponds to a field with an odd label l .

The results in (28) and (29) are easily combined into one equation, by observing that the additional sign only occurs for the ‘odd’ representations in the case that $N_\phi = (2N_e + n_{\text{qh}})/k$ is odd, thus

$$\text{td}(k, M=0, n_{\text{qh}}, N_e) = \sum_{l=0}^k (-1)^{l(2N_e+n_{\text{qh}})/k} \left(2 \cos\left(\frac{(l+1)\pi}{k+2}\right) \right)^{n_{\text{qh}}}. \quad (30)$$

To obtain the torus degeneracy for arbitrary M , we note that the only thing that changes is the possible values of b in the graph in Fig. 5. One can show that this gives rise to an additional factor of $(kM+2)/2$. Thus, we find (taking the possibility of quasiparticles into account as well)

$$\text{td}(k, M, n_{\text{qh}}, n_{\text{qp}}, N_e) = \left(\frac{kM+2}{2} \right) \sum_{l=0}^k (-1)^{l(2N_e+n_{\text{qh}}-n_{\text{qp}})/k} \left(2 \cos\left(\frac{(l+1)\pi}{k+2}\right) \right)^{n_{\text{qh}}+n_{\text{qp}}}. \quad (31)$$

The results presented here for the torus can be generalized to surfaces of arbitrary genus g . These results are presented in Appendix D, with the main result being (D1).

IV. CONCLUSIONS AND OUTLOOK

We considered the thin torus limit of the Read-Rezayi states. The ground state degeneracy on the torus is easily obtained in this limit. Elementary excitations correspond to domain walls between the various ground states. The problem of finding the number of degenerate states in the presence of elementary excitations translates to the combinatorial problem of finding all the domain walls of elementary charge. This particularly simple picture exactly reproduces the results one obtains by studying the fusion rules of the conformal field theory underlying the Read-Rezayi states. We provided explicit counting formulas for the degeneracy of the RR states on the torus. For completeness, we also give the results for surfaces of arbitrary genus.

The connection between the counting of domain walls and the fusion rules of the $su(2)_k$ conformal field theory describing the Read-Rezayi states can easily be extended to $su(n)_k$. The labels of the ground states correspond one-to-one to the extended labels of the representations of the $su(n)_k$ affine Lie algebra. The domain walls corresponding to quasiholes and -particles are interpreted as fusions with the representations ω_1 and ω_{n-1} respectively. That the elementary domain walls correctly reproduce these fusion rules is a consequence of the Littlewood-Richardson rule.

Acknowledgements. We wish to thank A. Karlhede and H. Hansson for fruitful discussions and for comments on this manuscript. J.K. was supported by a grant from the Swedish Research Foundation.

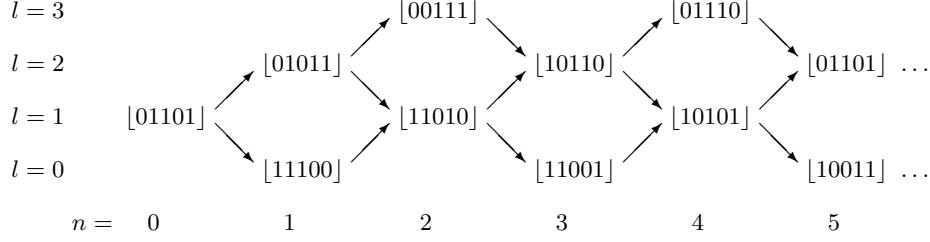


FIG. 7: A Bratteli diagram for $k = 3$ and $M = 1$ for sequences of quasiholes. Note how the ground states within each level are shuffled around among translated siblings. Note also that as for $M = 0$, each level l_1 has a complementary level $l_2 = k - l_1$ with translated siblings. For sequences of quasiparticles the structure of the diagram will be the same, but the sectors will follow each-other in a different order.

APPENDIX A: HIGHER M

Increasing M to $M \rightarrow M + 1$ corresponds to attaching one Jastrow factor, i.e. to push particles away from each-other. In the TT limit one should choose the term in the Jastrow factor that gives the particles the maximal spread. Up to an overall translation one has the following one-to-one correspondence: for the transition between $M = 0$ and $M = 1$ one has ($i, j \geq 0$)

$$|i_1, j_1, i_2, j_2, \dots\rangle_{M=0} \leftrightarrow |\underbrace{11\dots1}_i 0 \underbrace{11\dots1}_j 0 \underbrace{11\dots1}_i 0 \underbrace{11\dots1}_j 0 \dots\rangle_{M=1}. \quad (\text{A1})$$

The mapping applies for all M , for $M > 0$ resulting in the simple rule that every 1 in the pattern is replaced by 10 when increasing M by one. For example with $k = 3$:

$$|10110 \ 10110 \dots\rangle_{M=1} \leftrightarrow |10010100 \ 10010100 \dots\rangle_{M=2}. \quad (\text{A2})$$

In such a mapping domain walls of elementary charge are mapped to domain walls of elementary charge. Of course the absolute value of the charge of the domain wall will change. Hence, every state with quasiparticles and quasiholes for some higher M can (up to an overall translation) be one-to-one mapped to an $M = 0$ state with the same sequence of quasiparticles and quasiholes. The only change in the degeneracy is that the center of mass part of the degeneracy—related to the overall translations of a state—goes from $kM + 2$ to 2. The Bratteli diagrams will have the same topological structure (compare Fig. 7 and Fig. 1). A state keeps the same path in the diagram under the mapping and consequently the value of δ does not change. Hence the non-abelian part of the degeneracy counting will be the same. Note that for $M > 0$ the sectors within a level get shuffled around with translated siblings and therefore, in contrast to $M = 0$, the levels can no longer be labeled by specific unit cells. Note also that for $M > 0$ a domain wall has no longer the quasiparticle/quasihole ambiguity. The domain wall $[01101][01110]$ can only be an elementary quasiparticle, not also an elementary quasihole. This means that for quasiparticles, the sectors within each level in a Bratteli diagram get shuffled around in a different order compared to the same Bratteli diagram for quasiholes.

As for $M = 0$, the degeneracy formula (14) requires $\delta = 0$ when the sequences have to return to the initial level in the diagram ($l_2 = l_1$), whereas $\delta = 1$ is needed for the sequences which have to end with the complementary level ($l_2 = k - l_1$). Because increasing M for a given state neither changes the structure of the state in terms of whether one needs $\delta = 0$ or $\delta = 1$, nor changes the number of particles, quasiparticles and quasiholes, respectively, we have that $\delta = (N_e + n_{\text{qh}} - n_{\text{qp}})/k \bmod 2$ must apply also for $M \neq 0$. On the other hand, the equation $\delta = N_\phi \bmod 2$ applying for $M = 0$ changes to $\delta = N_\phi - MN_e \bmod 2$.

APPENDIX B: USING THE S -MATRIX TO COUNT CONFORMAL BLOCKS

The material presented in this section is standard (see, for instance, [43]), but is included for completeness. The Verlinde formula relates the fusion rules of the modular S -matrix in the following way: Let $(N_a)_{b,c}$ denote the number of times the operator ϕ_c appears in the fusion product of ϕ_a and ϕ_b , and $S_{a,b}$ the modular S -matrix. Then,

$$(N_a)_{b,c} = \sum_d \frac{S_{b,d} S_{a,d} S_{c,d}^*}{S_{1,d}}, \quad (\text{B1})$$

where the sum is over all fields, and $\mathbf{1}$ denotes the identity field. In other words, the S -matrix diagonalizes all the fusion matrices \mathbf{N}_a simultaneously; the eigenvalues of \mathbf{N}_a are $(\lambda_a)_d = S_{a,d}/S_{\mathbf{1},d}$, where d is any primary field;

$$\sum_{b,c} S_{b,d}^*(N_a)_{b,c} S_{c,e} = \frac{S_{a,d}}{S_{\mathbf{1},d}} \delta_{d,e} . \quad (\text{B2})$$

Note that S is unitary and symmetric.

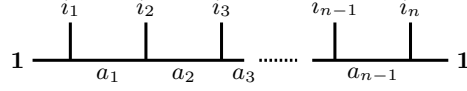


FIG. 8: The number of consistent labellings $\{a_i\}$ of this graph gives the number of conformal blocks on the plane.

First, we will apply this result to count the number of conformal blocks of the fields ϕ_i , $i = 1, \dots, n$ on the plane. This number is given by the number of labellings, consistent with the fusion rules, of the graph given in Fig. 8, namely

$$\#_{g=0} = \sum_{\{a_i\}} (N_{i_1})_{\mathbf{1},a_1} (N_{i_2})_{a_1,a_2} \cdots (N_{i_{n-1}})_{a_{n-2},a_{n-1}} (N_{i_n})_{a_{n-1},\mathbf{1}} .$$

Inserting the Verlinde formula (B1), and first performing the sum over the a_i , followed by the sums coming from (B1), we obtain

$$\#_{g=0} = \sum_a \frac{S_{i_1,a} S_{i_2,a} \cdots S_{i_n,a}}{(S_{\mathbf{1},a})^{n-2}} . \quad (\text{B3})$$

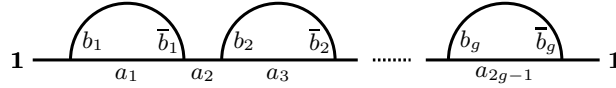


FIG. 9: The number of consistent labellings of this graph gives the degeneracy of a genus g surface.

We can now count the number of labellings on the graph in Fig. 9, which will give the number of states on the torus, if no fields (or quasiholes in our case) are present. We will make use of the result (B3) by choosing $i_{2j-1} = b_j$, $i_{2j} = \bar{b}_j$, for $j = 1, 2, \dots, g$, and performing a sum over all possible values of b_j . This leads to the following result:

$$\sum_a \left(\frac{1}{S_{\mathbf{1},a}} \right)^{2g-2} . \quad (\text{B4})$$

The genus g generalization of (B3) is given by

$$\#_g = \sum_a S_{i_1,a} \cdots S_{i_n,a} (S_{\mathbf{1},a})^{2-n-2g} , \quad (\text{B5})$$

as follows from gluing the graphs in Fig. 8 and Fig. 9 by summing over all intermediate states and making use of the unitarity of the S -matrix.

APPENDIX C: SOME DETAILS OF THE COUNTING IN SECTION III B

In this appendix, we will describe how to obtain the result (29), by making use of the results in the previous appendix. We start by first calculating the general result for the number of paths on the Bratteli diagram $d(k, n_{\text{qh}}, l_1, l_2)$. In terms of the fusion matrix \mathbf{N}_1 (recall that this matrix has the components $(N_1)_{i,j} = \delta_{i,j+1} + \delta_{i,j-1}$, for $i, j = 0, 1, \dots, k$), we have

$$d(k, n_{\text{qh}}, l_1, l_2) = (N_1^{n_{\text{qh}}})_{l_1, l_2} = \sum_{l=0}^k S_{l_1, l} \left(\frac{S_{1, l}}{S_{0, l}} \right)^{n_{\text{qh}}} S_{l_2, l} , \quad (\text{C1})$$

where the modular S -matrix for $su(2)_k$ is given by (see, for instance, [44])

$$S_{l_1, l_2} = \sqrt{\frac{2}{k+2}} \sin\left(\frac{(l_1+1)(l_2+1)\pi}{k+2}\right). \quad (\text{C2})$$

Thus, we obtain

$$d(k, n_{\text{qh}}, l_1, l_2) = \frac{2}{k+2} \sum_{l=0}^k \sin\left(\frac{(l+1)(l_1+1)\pi}{k+2}\right) \sin\left(\frac{(l+1)(l_2+1)\pi}{k+2}\right) \left(2 \cos\left(\frac{(l+1)\pi}{k+2}\right)\right)^{n_{\text{qh}}}. \quad (\text{C3})$$

Note that the eigenvalues of \mathbf{N}_1 are given by $S_{1,l}/S_{0,l} = 2 \cos\left(\frac{(l+1)\pi}{k+2}\right)$, which is a consequence of the Verlinde formula.

We can now perform the sum $\sum_{l=0}^k d(k, n_{\text{qh}}, l, k-l)$ explicitly by making use of

$$\sin\left(\frac{(l+1)(k-l_1+1)\pi}{k+2}\right) = (-1)^l \sin\left(\frac{(l+1)(l_1+1)\pi}{k+2}\right)$$

and the unitarity of the S -matrix. This gives the result stated in the main text (29):

$$\sum_{l=0}^k (-1)^l \left(2 \cos\left(\frac{(l+1)\pi}{k+2}\right)\right)^{n_{\text{qh}}}. \quad (\text{C4})$$

Note that one can also obtain the eigenvalues of the matrices \mathbf{N}_1 by observing that, as a function of k , the characteristic polynomials satisfy a recursion relation, which is the same as the recursion relation for the Chebyshev polynomials. The zeros of these polynomials are indeed the eigenvalues we quote above.

APPENDIX D: COUNTING RESULTS FOR ARBITRARY GENUS

For completeness, we give the state counting for arbitrary genus g . By making use of the results in Appendix B and C, we find

$$\text{td}(k, M, g, n_{\text{qh}}, n_{\text{qp}}, N_e) = \left(\frac{kM+2}{2}\right)^g \sum_{l=0}^k (-1)^{l(2N_e+n_{\text{qh}}-n_{\text{qp}})/k} \left(2 \cos\left(\frac{(l+1)\pi}{k+2}\right)\right)^{n_{\text{qh}}+n_{\text{qp}}} \left(\frac{k+2}{2 \sin\left(\frac{(l+1)\pi}{k+2}\right)^2}\right)^{g-1}. \quad (\text{D1})$$

Specializing to the case $g=1, n_{\text{qh}}=0$, we find that when $N_e=0 \pmod k$, the degeneracy is given by $(k+1)(kM+2)/2$. When $N_e=k/2 \pmod k$, which only occurs for k even, we find a degeneracy of $(kM+2)/2$. Some other simple results⁴, in the absence of quasiholes, are

$$\text{td}(2, M, g, 0, N_e) = ((2M+2)/2)^g 2^{g-1} (2^g + (-1)^{N_e}), \quad (\text{D2})$$

$$\text{td}(3, M, g, 0, N_e = 0 \pmod 3) = ((3M+2)/2)^g 2((5+\sqrt{5})^{g-1} + (5-\sqrt{5})^{g-1}), \quad (\text{D3})$$

$$\text{td}(4, M, g, 0, N_e = 0 \pmod 2) = ((4M+2)/2)^g (3^{g-1} + (-1)^{N_e/2} 2 \cdot 4^{g-1} + 2 \cdot 12^{g-1}). \quad (\text{D4})$$

In the case $g=0$, we reproduce the result that the degeneracy is given by the number of paths on the Bratteli diagram, namely $d(k, n_{\text{qh}}, 0, 0)$, or $d(k, n_{\text{qh}}, 0, k)$, (C3), for $(2N_e+n_{\text{qh}})/k=0 \pmod 2$ or $(2N_e+n_{\text{qh}})/k=1 \pmod 2$ respectively.

[1] R. B. Laughlin, Phys. Rev. Lett. **50**, 1395 (1983).

[2] G. Moore, and N. Read, Nucl. Phys. B **360**, 362 (1991).

[3] N. Read, and E.H. Rezayi, Phys. Rev. B **59**, 8084 (1999).

[4] M. Greiter, X.G. Wen, and F. Wilczek, Phys. Rev. Lett **66**, 3205 (1991); Nucl. Phys. B **374**, 567 (1992).

⁴ For $k=2, M=0$, these are known as the boundary condition sectors, or spin structures, of the genus g torus, as explained in [45].

- [5] R. L. Willet, J. P. Eisenstein, H. L. Störmer, D. C. Tsui, A. C. Gossard, and J. H. English, *Phys. Rev. Lett.* **59**, 1776 (1987).
- [6] R.H. Morf, *Phys. Rev. Lett.* **80**, 1505 (1998).
- [7] E. H. Rezayi, and F.D.M. Haldane, *Phys. Rev. Lett.* **84**, 4685 (2000).
- [8] G. Moller and S.H Simon, arXiv:0708.2680v1 (2007).
- [9] J.B. Miller *et.al.*, *Nature Phys.* **3**, 561 (2007).
- [10] E.H. Rezayi, and N. Read, cond-mat/060846 (2006).
- [11] See *eg*, M.H. Freedman, A. Kitaev, M. Larsen, and Z. Wang, *Bull. AMS.* **40**, 31 (2003); A. Kitaev, *Ann. Phys.* **303**, 2 (2003); S. Das Sarma, M. Freedman, C. Nayak, S.H. Simon, and A. Stern, arXiv:0707.1889v1 (2007).
- [12] P. Bonderson, and J.K. Slingerland, arXiv:0711.3204 (2007).
- [13] N.R. Cooper, N.K. Wilkin, and J.M.F. Gunn, *Phys. Rev. Lett.* **87**, 120405 (2001).
- [14] A. Cappelli, L.S. Georgiev, and I.T. Todorov, *Nucl. Phys. B* **599**, 499 (2001)
- [15] M. Oshikawa, Y.B. Kim, K. Shtengel, C. Nayak, and S. Tewari, *Ann. Phys.* **322**, 1477 (2007).
- [16] P.W. Anderson, *Phys. Rev. B* **28**, 2264 (1983).
- [17] W.P. Su, *Phys. Rev. B* **30**, 1069 (1984).
- [18] E.J. Bergholtz, and A. Karlhede, *J. Stat. Mech.* (2006) L04001.
- [19] E.J. Bergholtz, and A. Karlhede, arXiv:0712.1927 (2007).
- [20] E.J. Bergholtz, T. H. Hansson, M. Hermanns, and A. Karlhede, *Phys. Rev. Lett.* **99**, 256803 (2007).
- [21] E.J. Bergholtz, T.H. Hansson, M. Hermanns, A. Karlhede, and S. Viefers, arXiv:0712.3848 (2007).
- [22] A.Seidel, and K. Yang, arXiv:0801.2402 (2008).
- [23] E.J. Bergholtz, and A. Karlhede, *Phys. Rev. Lett.* **94**, 26802 (2005).
- [24] E.J. Bergholtz, J. Kailasvuori, E. Wikberg, T.H. Hansson, and A. Karlhede, *Phys. Rev. B* **74**, 081308(R) (2006).
- [25] A. Seidel, and D.-H. Lee, *Phys. Rev. Lett.* **97**, 056804 (2006).
- [26] N. Read, and E.H. Rezayi, *Phys. Rev. B.* **54**, 16864 (1996).
- [27] V. Gurarie, and E. Rezayi, *Phys. Rev. B* **61**, 5473 (2000).
- [28] P. Bouwknegt, and K. Schoutens, *Nucl. Phys. B* **547**, 501 (1999).
- [29] E. Ardonne, *J. Phys. A* **35**, 447 (2002).
- [30] N. Read, *Phys. Rev. B* **73**, 245334 (2006).
- [31] E. Ardonne, R. Kedem, and M. Stone, *J. Phys. A* **38**, 617 (2005).
- [32] B.A. Bernevig, and F.D.M. Haldane, arXiv:0707.3637 (2007).
- [33] B.A. Bernevig, and F.D.M. Haldane, arXiv:0711.3062 (2007).
- [34] F.D.M. Haldane, *Phys. Rev. Lett.* **55**, 2095 (1985).
- [35] R. Tao, and D.J. Thouless, *Phys. Rev. B* **28**, 1142 (1983).
- [36] W.P. Su, and J.R. Schrieffer, *Phys. Rev. Lett.* **46**, 738 (1981).
- [37] J.K. Slingerland, and F.A. Bais, *Nucl. Phys. B* **612**, 229 (2001).
- [38] E. Verlinde, *Nucl. Phys. B* **300**, 360 (1988).
- [39] A.B. Zamolodchikov, and V.A. Fateev, *Sov. Phys. JETP* **62**, 215 (1985).
- [40] D. Gepner, *Field identification in coset conformal field theories*, *Phys. Lett. B* **222**, 207 (1989).
- [41] M. Hermanns, H. Hansson and S. Viefers, unpublished.
- [42] E. Ardonne, and K. Schoutens, *Ann. Phys.* **322**, 201 (2007).
- [43] G. Moore, and N. Seiberg, *Lectures on RCFT*, in *Physics, Geometry and Topology*, H.C. Lee, ed., (Plenum Press, New York, 1990).
- [44] P. Di Francesco, P. Mathieu, and D. Sénéchal, *Conformal Field Theory*, (Springer, New York 1997).
- [45] N. Read, and D. Green, *Phys. Rev. B.* **61**, 10267 (2000).